

# The energy ratio mapping algorithm: A tool to improve the energy-based detection of odontocete echolocation clicks

Holger Klinck<sup>a)</sup> and David K. Mellinger

Cooperative Institute for Marine Resources Studies, Oregon State University and NOAA Pacific Marine Environmental Laboratory, 2030 Southeast Marine Science Drive, Newport, Oregon 97365

(Received 13 September 2010; revised 13 November 2010; accepted 29 November 2010)

The energy ratio mapping algorithm (ERMA) was developed to improve the performance of energy-based detection of odontocete echolocation clicks, especially for application in environments with limited computational power and energy such as acoustic gliders. ERMA systematically evaluates many frequency bands for energy ratio-based detection of echolocation clicks produced by a target species in the presence of the species mix in a given geographic area. To evaluate the performance of ERMA, a Teager-Kaiser energy operator was applied to the series of energy ratios as derived by ERMA. A noise-adaptive threshold was then applied to the Teager-Kaiser function to identify clicks in data sets. The method was tested for detecting clicks of Blainville's beaked whales while rejecting echolocation clicks of Risso's dolphins and pilot whales. Results showed that the ERMA-based detector correctly identified 81.6% of the beaked whale clicks in an extended evaluation data set. Average false-positive detection rate was 6.3% (3.4% for Risso's dolphins and 2.9% for pilot whales). © 2011 Acoustical Society of America. [DOI: 10.1121/1.3531924]

PACS number(s): 43.30.Sf, 43.80.Ev [WWA]

Pages: 1807–1812

## I. INTRODUCTION

As equipment costs have fallen, acoustic methods have been used increasingly to detect, locate, and track marine mammals (Mellinger *et al.*, 2007). Widespread use of these methods has led to a flood of digital data, which in turn has necessitated the development of automated techniques for analyzing these data, particularly for automated detection of marine mammal vocalizations (Desharnais and Hay, 2004; Adam *et al.*, 2006; Moretti *et al.*, 2008; Pavan *et al.*, 2010). One family of methods that has gained widespread use for such detection is measuring the signal level or signal energy in a certain frequency band over a short time period—sometimes just one sample interval (Gillespie, 1997)—and comparing this instantaneous sum to its long-term average. This method, which we term the *band-limited energy sum*, has been used for detecting echolocation clicks of many odontocete species, including sperm whales (*Physeter macrocephalus*; Gillespie, 1997), finless porpoises (*Neophocaena phocaenoides*; Akamatsu *et al.*, 2001), harbor porpoises (*Phocoena phocoena*; Gillespie and Chappell, 2002), and many species of delphinids (Kim *et al.*, 2006). Echolocation clicks are used for navigation, prey detection, and communication and are the predominant vocalizations of toothed whales. For this reason and the fact that several odontocete species, such as sperm whales and beaked whales, do not or only rarely produce tonal sounds (“whistles”), echolocation clicks are appropriate target signals to detect their presence.

A significant advantage of the band-limited energy sum detection methods is the fact that they can operate in the time domain by employing time-domain digital or analog filters, avoiding the computational expense of a discrete Fourier

transform or other spectrum estimators. The savings in processing effort, and hence energy use, can be important for battery-operated instruments that operate autonomously for long periods of time, including devices specialized for detecting odontocete echolocation clicks (e.g., the C-POD, Chelonia Ltd., Cornwall, UK), instruments that detect and record wide varieties of vocalizations (Anagnostou *et al.*, 2011), and ocean gliders and floats equipped with real-time acoustic detection capability (Klinck *et al.*, 2009; Olmstead *et al.*, 2010).

A variant of these methods is to calculate the ratio of signal energies in two frequency bands. This technique, which we term the *band-limited energy ratio*, is useful for species-specific detection—for detecting clicks of those species with distinctive spectral-level differences between the two frequency bands while rejecting clicks of other species. It has been used for detection of harbor porpoises (e.g., Thomsen *et al.*, 2005; Verfuss *et al.*, 2007), which have a distinctive spectral peak above 100 kHz (Au *et al.*, 1999). Numerous other odontocete species have been found to have distinctive spectral peaks and notches (e.g., Johnson *et al.*, 2004; Soldevilla *et al.*, 2008) that could be exploited for species-specific detection in the time domain. In many cases, however, constructing a species-specific click detector requires knowledge not only of the desired species' click spectra but also of the click spectra of other species that may be present, so that the appropriate frequency bands are used in calculating the energy ratio.

Also of importance for echolocation click detection are the spectral differences between on-axis and off-axis clicks (e.g., Au, 1993). A detection algorithm is most useful if it can detect clicks emitted at any angle from the desired species. For a band-limited energy ratio detector that uses digital filtering, the filter's order (length of its coefficient vector) affects the rapidity of attenuation as a function of frequency and hence affects the effective width of the frequency bands used

<sup>a)</sup>Author to whom correspondence should be addressed. Electronic mail: Holger.Klinck@oregonstate.edu

in the ratio. Thus filter order is a tunable parameter for developing an effective detector.

Here we present an algorithm, the *energy ratio mapping algorithm* (ERMA), for choosing the filter frequencies for a band-limited energy ratio detector. ERMA uses the normalized spectrum of the desired species, as well as spectra of selected non-desired species present in the same geographic area, to arrive at efficient filter parameters for time-domain detection of echolocation clicks. The method is tested for detecting clicks of Blainville's beaked whales (BBWs) (*Mesoplodon densirostris*) while rejecting echolocation clicks of Risso's dolphins (RDs) (*Grampus griseus*) and short-finned pilot whales (SPWs) (*Globicephala macrorhynchus*).

## II. METHODS

The echolocation click spectra of most species of odontocetes show species-specific characteristics at certain frequencies, including rises, notches, and peaks. Soldevilla *et al.* (2008), for instance, found such spectral differences among echolocation clicks of five species of delphinids, and Johnson *et al.* (2006) found a characteristic rise in energy between approximately 20 and 30 kHz in clicks of BBWs. This feature, which in BBWs is robust to changes in off-axis angle (Johnson *et al.*, 2006), can be exploited for the detection of this species by calculating the ratio between the energy in two frequency bands, one above and one below the rise. A detection method based on such energy ratios would not be triggered by, for example, vocalizing sperm whales, because the peak frequency of sperm whale echolocation clicks occurs at lower frequencies, approximately 11 kHz (Møhl *et al.*, 2003). However, many species of the family Delphinidae produce echolocation clicks with similar spectral characteristics to those of BBWs and here the discrimination becomes more difficult. The goal of this study was to develop a tool to maximize the performance of energy ratio-based detectors for odontocete echolocation clicks in the time domain and to minimize the false-positive detection rate.

The detection distance of passive acoustic monitoring (PAM) systems is rather limited for high frequency sounds like echolocation clicks, principally because these sounds are rapidly attenuated in seawater (e.g., Urick, 1983; Zimmer *et al.*, 2008). Accordingly, PAM packages capture echoloca-

tion clicks of species which occur in closer vicinity of the deployment location. This implies that depending on the deployment location of the PAM package, only species common at the field site—the *geographic species mix*—potentially interfere with the detection of a target species. This fact must be taken into consideration when designing detection and classification methods. Note that the available data sets for RDs and SPWs were actually recorded within different geographic areas. However, as the geographical distribution of these species and BBWs potentially overlaps, the authors believe it is valid to refer to RDs and SPWs as the geographic species mix in the following paragraphs.

ERMA was developed to systematically evaluate the frequency bands for energy ratio-based detection of echolocation clicks produced by a target species in the presence of a given geographic species mix. The data set used here to train and test ERMA (Table I) is a subsample of the data set provided for the Third International Workshop on Detection, Classification, and Localization of Marine Mammals using Passive Acoustics (data available at www.MobySound.org). All data sets are sampled at 96 kHz with 16-bit sample resolution. The analyzed data sets were recorded in the Bahamas at the U.S. Navy's Atlantic Undersea Test and Evaluation Center (AUTEK) and in the Southern California Offshore Range (SCORE). As the passive acoustic surveillance systems of AUTEK and SCORE are similar, spectrum differences between species should not merely be the result of different hydrophones or analog-to-digital conversion systems. The recordings (Table I) were hand-labeled by analysts to delineate the time and frequency as well as signal-to-noise ratio (SNR) of all echolocation clicks present. These sound files and metadata provide ground-truth data for BBW (the target species), RD, and SPW echolocation clicks.

In total, 2474 BBW clicks, 5948 RD clicks, and 9255 SPW clicks were labeled within the test data sets (see Table I). These numbers actually represent the number of 10 ms data intervals containing clicks, as the detector (see below) is incapable of separating multiple clicks within a 10 ms data chunk. The mean band-limited (10–40 kHz) SNR of the labeled BBW clicks was  $12.6 \pm 4.1$  dB, of the RD clicks was  $9.7 \pm 3.9$  dB, and of the SPW clicks was  $12.2 \pm 3.3$  dB.

In its first step, ERMA analyzed the spectral characteristics of the echolocation clicks of the target species (BBW) and those of the geographic species mix (RD and SPW). In

TABLE I. Overview of the data set used to train and test ERMA. It comprises a subsample of the data set for the Third International Workshop on the Detection, Classification and Localization of Marine Mammals Using Passive Acoustics, Boston, MA, USA; published online at www.MobySound.org. All recordings are sampled at 96 kHz and 16-bit resolution.

| Data set   | Hydrophone <sup>a</sup> | Date/time <sup>b</sup> | Duration | Species | Train/test |
|--|-------------------------|------------------------|----------|---------|------------|
| Set3_A3_042705_H27_A0500-0530-1410-1440loc_1330-1500min.wav          | A-H27                   | 27.04.2005/18:10:00    | 90 s     | BBW     | Train      |
| Set3_A3_042705_H26_A0230-0300-1140-1210loc_2130-2330min.wav          | A-H26                   | 27.04.2005/15:40:00    | 65 s     | BBW     | Train      |
| Set4-A6-092705-H76-0155-0214-1030-1049loc_0300-0600min.wav           | A-H76                   | 27.09.2005/14:30:36    | 180 s    | BBW     | Test       |
| Set4-A7-092705-H84-0155-0214-1030-1049loc_0230-0430min.wav           | A-H84                   | 27.09.2005/14:30:36    | 120 s    | BBW     | Test       |
| Set6-A8-H86-081906-0030-0100-0745-0815loc_3-6min.wav                 | S-H86                   | 19.08.2006/14:45:40    | 180 s    | RD      | Train      |
| Set3-A5-H54-081606-0230-0300-0847-0917loc_1340-6600.wav <sup>c</sup> | S-H54                   | 16.08.2006/16:01:34    | 300 s    | RD      | Test       |
| Set3-A2-092605-H23-0615-0630-1450-1505loc_0800-1000min.wav           | A-H23                   | 26.09.2005/18:50:30    | 120 s    | SPW     | Train      |
| Set7-A1-096605-H01-0030-0100-0846-0916loc_9-19min.wav                | A-H01                   | 30.09.2005/12:46:40    | 600 s    | SPW     | Test       |

<sup>a</sup>A, AUTEK hydrophone; S, SCORE hydrophone.

<sup>b</sup>Time stamp of file in UTC.

<sup>c</sup>The first 300 s of the file were analyzed.

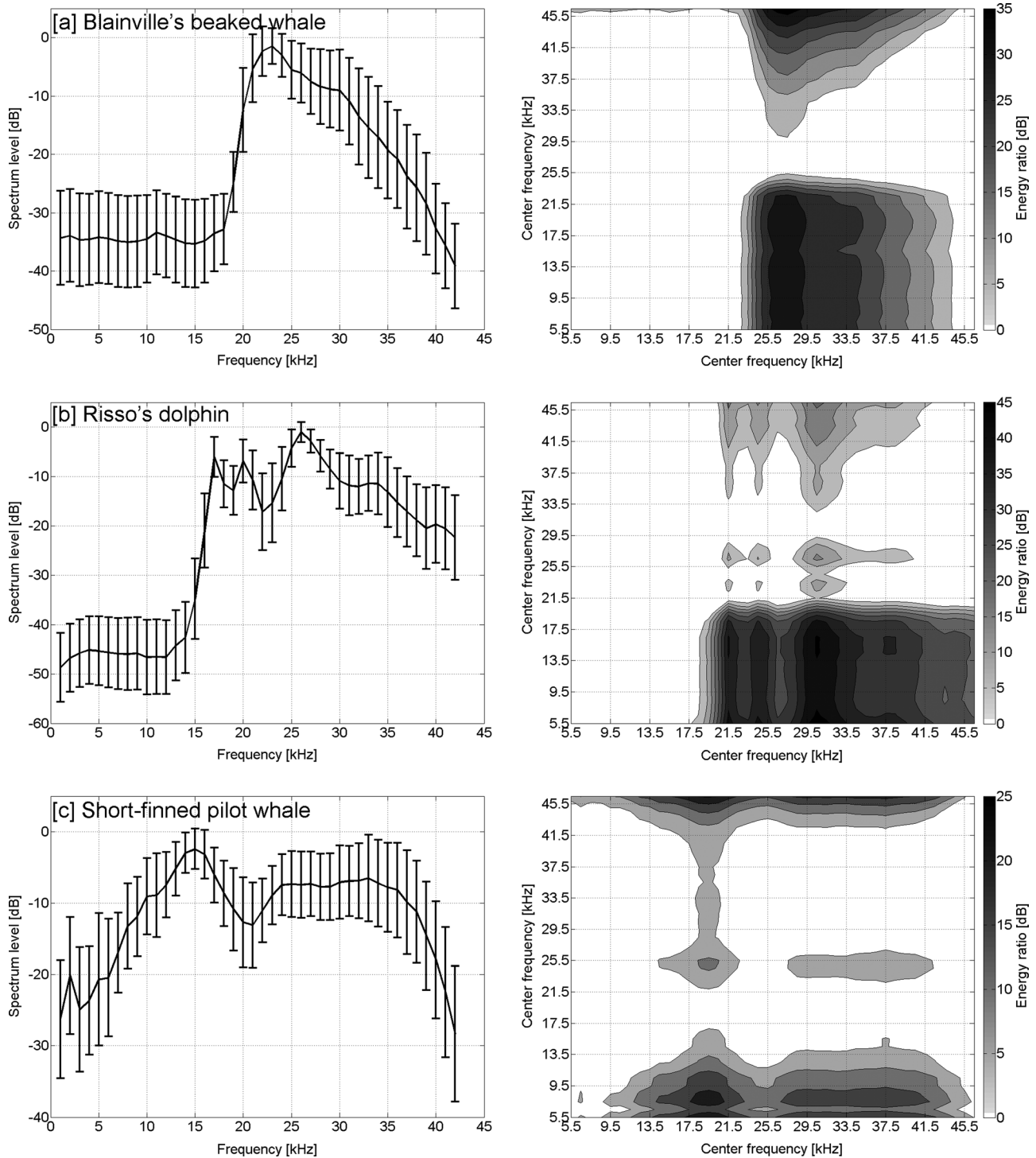


FIG. 1. Normalized power spectrum (left) and corresponding energy ratio map (right) for (a) BBW ( $n = 279$ ), (b) RD ( $n = 429$ ), and (c) SPW ( $n = 389$ ). Vertical bars in the normalized power spectra represent standard deviation for corresponding energy in frequency bin.

total, 279 BBW clicks, 429 RD clicks, and 389 SPW clicks were manually extracted from the training data sets and used for this analysis. All clicks used in this step of the analysis exceeded a band-limited (10–40 kHz) SNR of 15 dB. ERMA then applied a filter bank consisting of 43 Butterworth filters (BFs) (fifth-order band-pass filters with 1 kHz between corner frequencies; center frequencies spaced evenly from 5.5 to 47.5 kHz) to all samples. After applying the filter bank, energy ratios were calculated for all possible filter pairs. The results are shown in Fig. 1.

Figure 1(a) shows the normalized power spectrum (left) and the resulting energy ratio map (right) for BBW—the *target species map*—while Figs. 1(b) and 1(c) show the power spectra and *non-target species maps* for RD and SPW. As described in Johnson *et al.* (2006), the rise in energy starting at approximately 20 kHz is the most prominent spectral feature of the BBW echolocation clicks. In contrast, RD echolocation clicks [Fig. 1(b)] show a more complex spectral structure, with energy peaks and notches at species-specific frequencies (Soldevilla *et al.*, 2008). Echolocation clicks of

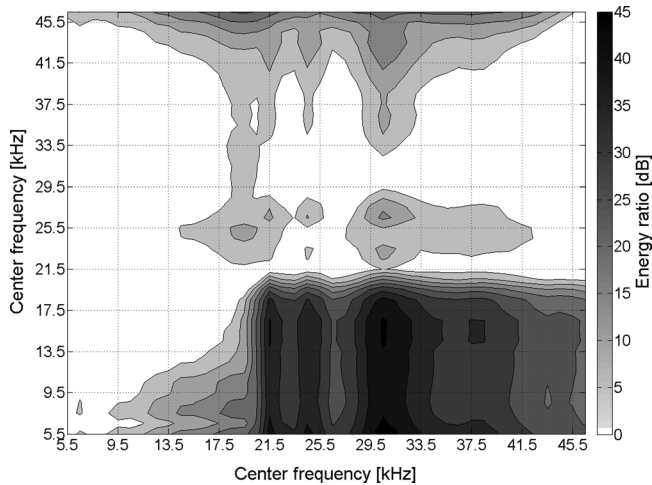


FIG. 2. ERMA combined non-target species map for RD and SPW.

SPW [Fig. 1(c)] show significant energy at frequencies below 20 kHz.

The energy ratio map for BBW [Fig. 1(a)] shows that the area of highest ratios is broad and covers the center frequency bins 24–33 kHz and 5.5–22.5 kHz. For detection purposes, one solution could be to calculate the energy ratio between the frequencies 24–33 kHz and 12–21 kHz. However, as RD echolocation clicks show a similar overall energy distribution as BBW, a detector based on these ratios would not be able to distinguish between the two species; such a detector would suffer from a high false-alarm (false-positive) rate.

To improve detection performance and to reduce false-alarm rates, ERMA calculates, in a second step, a *combined non-target species map* (Fig. 2) by taking the maximum at each grid point over all non-target species maps (here, RD and SPW). Figure 2 shows that the combined non-target species map is dominated by the RD map because of overall higher energy ratios. SPWs are more broad-band and cover a wider frequency range; accordingly, energy ratios are lower. However, the effects of the SPW map are visible in the combined non-target species map at frequencies below 20 kHz.

In the third and final step, ERMA subtracts the combined non-target species map (Fig. 2) from the target species map [Fig. 1(a)], producing the resulting *discrimination map* shown in Fig. 3. The position of this map's peak in  $X$  and  $Y$  corresponds to the optimum numerator and denominator frequencies, respectively, for discriminating the target species from the other species in the geographic species mix.

An energy ratio detector using the frequency bands produced by ERMA—the *ERMA detector*—was applied to the test data sets to evaluate the performance of the ERMA approach for detection of BBW echolocation clicks and rejection of non-target species' clicks. As a comparison, a similar detector—the *comparison detector*—was constructed using frequency bands based on only the target species map [Fig. 1(a)] and was tested on the same sounds and compared to the ERMA results.

The ERMA detector worked as follows. The input signal  $x(t)$ , with range  $\pm 1$ , was filtered with two second-order band-pass Butterworth filters BF1 and BF2 to produce filtered signals  $x_1(t)$  and  $x_2(t)$ . These are windowed with a 10 ms rectangular

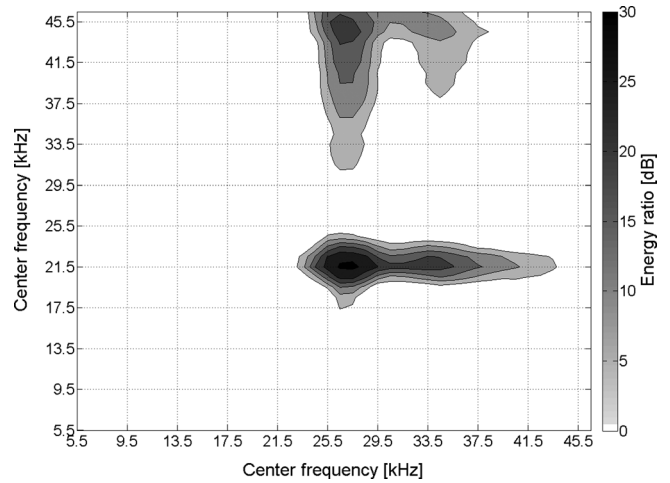


FIG. 3. ERMA discrimination map for BBW with consideration of two additional odontocete species, RD and SPW.

window to produce a stream of filtered data chunks of 10 ms duration at a rate of 100 chunks per second, and the energy ratio  $e(n)$  for each chunk in decibel is calculated

$$e(n) = 20 \log_{10} \frac{\max |x_1(n)|}{\max |x_2(n)|}.$$

If  $e(n)$  was less than zero, it was set to zero.

In a second step, a Teager-Kaiser energy operator (Kaiser, 1990; Kandia and Stylianou, 2006) was applied to  $e(n)$  to produce a detection function  $d(n)$

$$d(n) = e(n)^2 - e(n+1)e(n-1).$$

A detection threshold  $t_d$  was calculated dynamically for 60 s intervals, applied to the detection function, and clicks were identified as times when  $d(n)$  exceeds  $t_d$ . The formula to calculate the detection threshold is

$$t_d = \frac{f_c}{\left| \log_{10} \frac{\text{mean}_{n \leq n_i < n+60s} \max_i |x_2(n_i)| \right|}$$

which was based on the energy level in the frequency band of BF2 and was determined heuristically by repeated analysis of the BBW training data set. Factor  $f_c$ , a constant that scales the log mean to achieve an effective threshold, was set such that 95% of the manually extracted echolocation BBW clicks exceeding a SNR (>15 dB) from the training data set were detected.

The comparison detector used a similar procedure, but the corner frequencies of its band-pass filters were based on only the target species map [Fig. 1(a)]. The performance of each detector was evaluated by comparing the time stamps of the detections with the time stamps of the manually labeled clicks. A detection was counted when the time of a labeled click fell within the time span of a 10 ms chunk as detected by the system.

### III. RESULTS

The discrimination map (Fig. 3) indicated the best frequency bands (BF1: 26–28 kHz and BF2: 19.5–21.5 kHz)

TABLE II. Detector performance comparison.

| ERMA <sup>a</sup> | $f_c^b$ | BBW<br>( $n=2474$ ) | RD<br>( $n=5948$ ) | SPW<br>( $n=9255$ ) | Correct<br>detection<br>rate (%) | Average<br>false-<br>positive<br>rate (%) |
|-------------------|---------|---------------------|--------------------|---------------------|----------------------------------|---|
| No                | 110     | 1548                | 2138               | 284                 | 62.6                             | 13.7                                      |
| Yes               | 170     | 2018                | 600                | 504                 | 81.6                             | 6.3                                       |

<sup>a</sup>Frequency bands detector: no = 24–33 kHz and 12–21 kHz; yes = 26–28 kHz and 19.5–21.5 kHz.

<sup>b</sup> $f_c$  = factor used in the detection threshold formula.

for calculating a ratio to detect the BBW clicks in the presence of interfering RD and SPW echolocation clicks. Frequency band BF1 covered one of the spectral notches of the RD and the SPW echolocation clicks and BF2 covered one of the spectral peaks of the SPW echolocation clicks [see Figs. 1(b) and 1(c)]. The comparison detector, which did not consider RD and SPW, used energy ratios of the frequency bands 24–33 kHz and 12–21 kHz, which cover essentially the entire BW ratio peak [Fig. 1(a)].

Table II shows the results of these two approaches. The comparison detector found 62.6% of all BBW clicks in the test data sets, with an average false-positive detection rate of 13.7%. Although false-positive detections triggered by SPW were negligible (3.1%), as might be expected from its broad-spectrum energy peak, almost 36% of the RD clicks were detected. The use of the ERMA-derived frequency bands reduced the overall false-positive detection rate to 6.3% (7.4% lower) and significantly increased the correct detection rate by almost 30%. The increase of the BBW detection rate is largely caused by the narrower bandwidth of the filter pair which allows for detection of lower SNR clicks. In total, 2018 (81.6%) of the BBW clicks, 600 (10.1%) RD clicks, and 504 (5.5%) SPW clicks were detected by the optimized detector. The results were also used to generate receiver operating characteristic (ROC) curves for the ERMA detector, shown in Fig. 4.

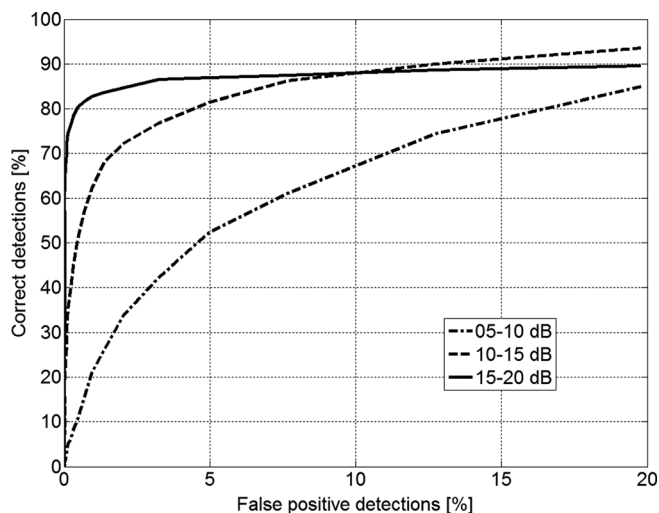


FIG. 4. ROC curves for ERMA-based detector for BBW and SNR classes 5–10 dB, 10–15 dB, and 15–20 dB.

## IV. DISCUSSION

ERMA allows users to objectively choose efficient frequency bands to detect a target species while taking into account a geographic species mix. The results presented here indicate that the ERMA method increases the performance of energy-based odontocete click detection by reducing the number of false-positive detections caused by non-target species. This is especially helpful for applications in low-power computing environments, particularly battery-powered oceanographic platforms such as acoustic gliders in which sophisticated detection/classification algorithms cannot be operated continuously. However, because of the number of false-positive detections, the ERMA detector may work best when used as the first step of a two-step identification system; the second step could be a significantly more sophisticated classifier (e.g., Roch *et al.*, 2011) that improves detection performance. Such classifiers are typically quite computationally intensive and are best used on only a tiny fraction of the input sound signal. By reducing the number of clicks which are sent to the second-step classifier, the ERMA detector reduces the computational cost of the overall process.

In detection and classification, overfitting can be a significant problem, particularly when large numbers of parameters are involved in the detector or classifier (Duda *et al.*, 2001). Overfitting in general occurs when the degrees of freedom in parameter selection exceed the information content of the data which leads to arbitrariness in the final model parameters. As a result, a model can fit the training data set very well but does poorly when applied to a new data set; overfitting is essentially a reduced ability to generalize. The ERMA detector is principally parameterized with only five numbers—the lower and upper frequencies of BF1 and BF2 and the detection threshold  $t_d$ —and thus is less prone to over-training than many other methods.

An additional step that could improve performance would be to use information about the inter-click interval (ICI) of clicks in the acoustic signal. Cuvier’s and Blainville’s beaked whales for instance, click at intervals of approximately 0.2–0.5 s (Johnson *et al.*, 2004, 2006; Zimmer *et al.*, 2005), slower than click rates of Risso’s dolphins (Madsen *et al.*, 2004) and other pilot whales (Weilgart and Whitehead, 1990). A system that incorporated ICI information could potentially have better performance than the raw algorithm presented here. ICIs can be difficult to calculate when multiple animals are present, but recent methods offer promise for separating click trains of individuals (Baggenstoss, 2008) and thus making ICI measurement relatively simple.

It is hoped that ERMA or extensions of it will soon be used for real-time detection of beaked whales and other species of concern, especially for mitigation of harm to these species by human activities.

## ACKNOWLEDGMENTS

Thanks to Dave Moretti and his team for collecting the data sets and making them available. Thanks also to Karolin Klinck and Sara Heimlich for labeling the data. We also thank two anonymous reviewers for helpful comments on the

previous version of the manuscript. This work was supported by Naval Postgraduate School grants N00244-08-1-0029, N00244-09-1-0079, and N00244-10-1-0047, and Office of Naval Research grants N00014-08-1-1082, N00014-10-1-0387, and N00014-08-1-1198. This is NOAA/PMEL contribution #3607.

- Adam, O., Motsch, J. F., Desharnais, F., DiMarzio, N., Gillespie, D., and Gisiner, R. C. (2006). "Overview of the 2005 workshop on detection and localization of marine mammals using passive acoustics," *Appl. Acoust.* **67**, 1061–1070.
- Akamatsu, T., Wang, D., Wang, K., and Wei, Z. (2001). "Comparison between visual and passive acoustic detection of finless porpoises in the Yangtze River, China," *J. Acoust. Soc. Am.* **109**, 1723–1727.
- Anagnostou, M. N., Nystuen, J. A., Anagnostou, E. N., Papadopoulos, A., and Lykousis, V. (2011). "Passive aquatic listener (PAL): An adoptive underwater acoustic recording system for the marine environment," *Nucl. Instrum. Methods Phys. Res. A* **626–627**, Suppl. 1, S94–S98.
- Au, W. W. L. (1993). *The Sonar of Dolphins* (Springer-Verlag, New York), pp. 104–113.
- Au, W. W. L., Kastelein, R. A., Rippe, T., and Schooneman, N. M. (1999). "Transmission beam pattern and echolocation signals of a harbor porpoise (*Phocoena phocoena*)," *J. Acoust. Soc. Am.* **106**, 3699–3705.
- Baggenstoss, P. M. (2008). "Joint localization and separation of sperm whale clicks," *Can. Acoust.* **36**, 125–131.
- Desharnais, F., and Hay, A. E. (2004). "Overview of the 2003 workshop on detection and localization of marine mammals using passive acoustics," *Can. Acoust.* **32**, 9–16.
- Duda, R. O., Hart, P. E., and Stork, D. G. (2001). *Pattern Classification*, 2nd ed. (Wiley, New York), pp. 5 and 16.
- Gillespie, D. (1997). "An acoustic survey for sperm whales in the Southern Ocean Sanctuary conducted from the RSV Aurora Australis," *Rep. Int. Whal. Comm.* **47**, 897–907.
- Gillespie, D., and Chappell, O. (2002). "An automatic system for detecting and classifying the vocalisations of harbour porpoises," *Bioacoustics* **13**, 37–61.
- Johnson, M. P., Madsen, P. T., Zimmer, W. M. X., Aguilar de Soto, N., and Tyack, P. L. (2004). "Beaked whales echolocate on prey," *Proc. R. Soc. London* **271**, S383–S386.
- Johnson, M. P., Madsen, P. T., Zimmer, W. M. X., Aguilar de Soto, N., and Tyack, P. L. (2006). "Foraging Blainville's beaked whales (*Mesoplodon densirostris*) produce distinct click types matched to different phases of echolocation," *J. Exp. Biol.* **209**, 5038–5050.
- Kaiser, J. F. (1990). "On a simple algorithm to calculate the 'energy' of a signal," in *Proceedings of the IEEE International Conference on Acoustics, Speech, and Signal Processing, ICASSP-'90*, Albuquerque, NM, pp. 381–384.
- Kandia, V., and Stylianou, Y. (2006). "Detection of sperm whale clicks based on the Teager-Kaiser energy operator," *Appl. Acoust.* **67**, 1144–1163.
- Kim, K. H., Hursky, P., Porter, M. B., Hildebrand, J. A., Henderson, E. E., and Wiggins, S. M. (2006). "Automated passive acoustic tracking of dolphins in free-ranging pods," in *Proceedings of the Eighth European Conference on Underwater Acoustics*, Carvoeiro, Portugal, edited by S. M. Jesus and O. C. Rodriguez, pp. 329–334.
- Klinck, H., Mellinger, D. K., Bogue, N. M., Luby, J. C., Jump, W. A., Pyle, J. M., and Shilling, G. B. (2009). "Autonomous passive acoustic monitoring of marine mammals using the Seaglider: Onboard real-time detection and classification of target signals," *ONR Marine Mammal Program Review*, December 7–10, Alexandria, VA, p. 86.
- Madsen, P. T., Kerr, I., and Payne, R. (2004). "Echolocation clicks of two free-ranging, oceanic delphinids with different food preferences: False killer whales *Pseudorca crassidens* and Risso's dolphins *Grampus griseus*," *J. Exp. Biol.* **207**, 1811–1823.
- Mellinger, D. K., Stafford, K. M., Moore, S. E., Dziak, R. P., and Matsumoto, H. (2007). "An overview of fixed passive acoustic observation methods for cetaceans," *Oceanogr.* **20**, 36–45.
- Möhl, B., Wahlberg, M., Madsen, P. T., Heerfordt, A., and Lund A. (2003). "The monopulsed nature of sperm whale clicks," *J. Acoust. Soc. Am.* **114**, 1143–1154.
- Moretti, D., DiMarzio, N., Morrissey, R., Mellinger, D. K., Heimlich, S. L., and Pettis, H. (2008). "Overview of the 3rd international workshop on the detection and classification of marine mammals using passive acoustics," *Can. Acoust.* **36**, 7–11.
- Olmstead, T. J., Roch, M. A., Hursky, P., Porter, M. B., Klinck, H., Mellinger, D. K., Helble, T., Wiggins, S. M., D'Spain, G. L., and Hildebrand, J. A. (2010). "Autonomous underwater glider based embedded real-time marine mammal detection and classification," *J. Acoust. Soc. Am.* **127**, 1971(A).
- Roch, M. A., Klinck, H., Baumann-Pickering, S., Mellinger, D. K., Qui, S., Soldevilla, M. S., and Hildebrand, J. A. (2011). "Classification of echolocation clicks from odontocetes in the Southern California Bight," *J. Acoust. Soc. Am.* **129**, 467–475.
- Pavan, G., Adam, O., and Thomas, L. (2010). *Proceedings of the 4th International Workshop on Detection, Classification and Localization of Marine Mammals Using Passive Acoustics and 1st International Workshop on Density Estimation of Marine Mammals Using Passive Acoustics*, September 2009, 10–13, University of Pavia, Collegio Cairoli, Italy, *Appl. Acoust.* **71**, 991–993.
- Soldevilla, M. S., Henderson, E. E., Campbell, G. S., Wiggins, S. M., Hildebrand, J. A., and Roch, M. A. (2008). "Classification of Risso's and Pacific white-sided dolphins using spectral properties of echolocation clicks," *J. Acoust. Soc. Am.* **124**, 609–624.
- Thomsen, F., Van Elk, N., Brock, V., and Werner, P. (2005). "On the performance of automated porpoise-click detectors in experiments with captive harbour porpoises (*Phocoena phocoena*)," *J. Acoust. Soc. Am.* **118**, 37–40.
- Urick, R. J. (1983). *Principles of Underwater Sound* (McGraw-Hill, New York), pp. 102–111.
- Verfuss, U. K., Honnef, C. G., Meding, A., Daehne, M., Mundry, R., and Benke, H. (2007). "Geographical and seasonal variation of harbour porpoise (*Phocoena phocoena*) presence in the German Baltic Sea revealed by passive acoustic monitoring," *J. Mar. Biol. Assoc. U.K.* **87**, 165–176.
- Weilgart, L. S., and Whitehead, H. (1990). "Vocalizations of the North Atlantic pilot whale (*Globicephala melas*) as related to behavioral contexts," *Behav. Ecol. Sociobiol.* **26**, 399–402.
- Zimmer, W. M. X., Harwood, J., Tyack, P. L., Johnson, M. P., and Madsen, T. P. (2008). "Passive acoustic detection of deep-diving beaked whales," *J. Acoust. Soc. Am.* **124**, 2823–2832.
- Zimmer, W. M. X., Johnson, M. P., Madsen, T. P., and Tyack, P. L. (2005). "Echolocation clicks of free-ranging Cuvier's beaked whales (*Ziphius cavirostris*)," *J. Acoust. Soc. Am.* **117**, 3919–3927.